

# SUPPORTING INFORMATION

## Sodium site occupancy and phosphate speciation in natrophosphate are invariant to changes in NaF and Na<sub>3</sub>PO<sub>4</sub> concentration

Trent R. Graham,<sup>A,\*</sup> Emily T. Nienhuis,<sup>A</sup> Jacob G. Reynolds,<sup>B</sup>  
Jose Marcial,<sup>A</sup> John S. Loring,<sup>A</sup> Kevin M. Rosso,<sup>A</sup> and Carolyn I. Pearce<sup>A,C</sup>

<sup>A</sup> Pacific Northwest National Laboratory, Richland, Washington 99352, United States

<sup>B</sup> Washington River Protection Solutions, LLC, Richland, Washington 99352, United States

<sup>C</sup> Department of Crop and Soil Sciences, Washington State University, Pullman, Washington 99164, United States

### CORRESPONDING AUTHOR

\* Trent R. Graham, E-mail: [trenton.graham@pnl.gov](mailto:trenton.graham@pnl.gov)

## 1.0 FIGURES

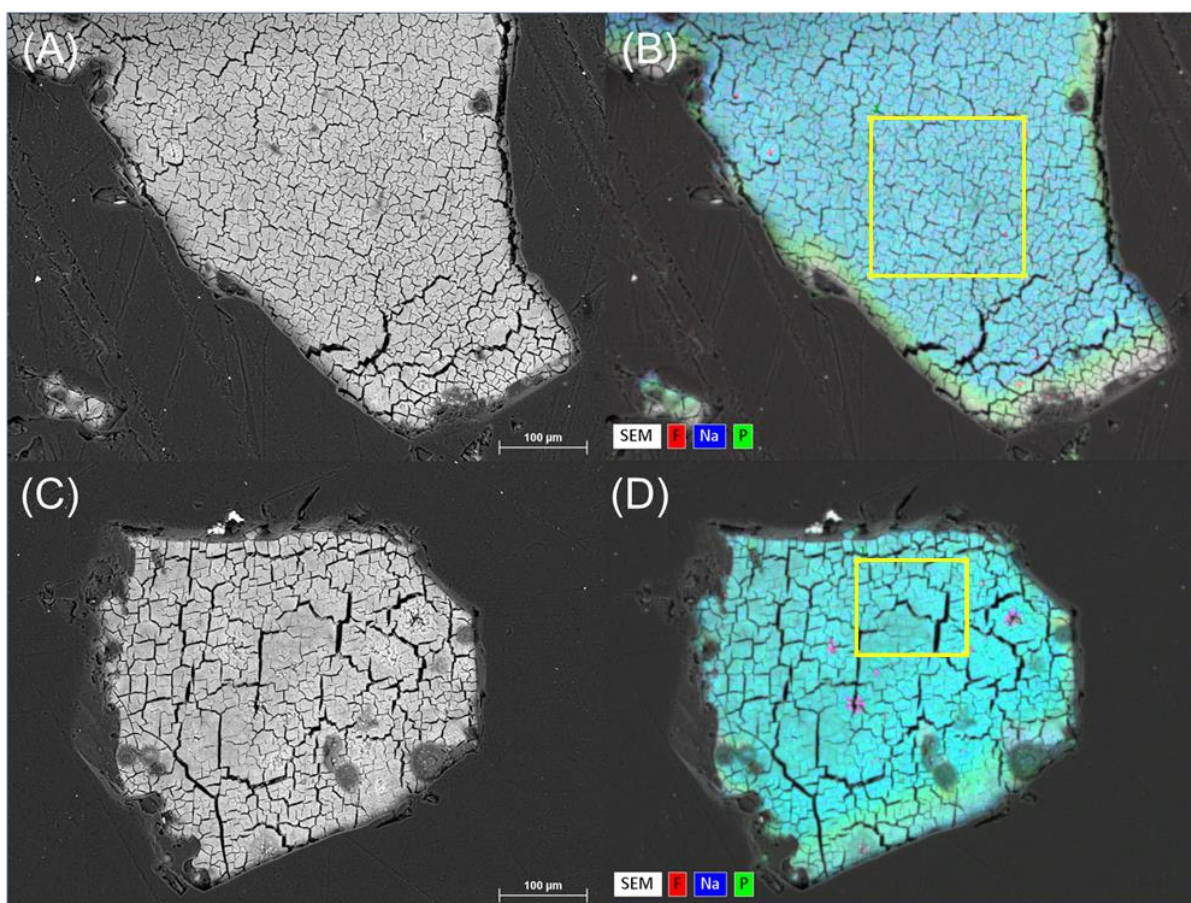


**Figure S1.** Measurement of elemental composition of natrophosphate synthesized under F-poor conditions and F-rich conditions. (A) The scanning electron microscopy (SEM) and the (B) SEM energy dispersive X-ray spectroscopy (EDS) of natrophosphate synthesized under F-poor conditions are shown. (C) The SEM and the (D) SEM EDS of natrophosphate synthesized under F-rich conditions are shown. The area selected for quantification of composition are annotated in yellow. The results from the quantification are shown in Figure S2. Note, localized regions relatively enriched in fluoride are apparent in the F-rich sample. These regions are hypothesized to be due to evaporation of residual mother liquor. The presence of mother liquor occlusions is consistent with the observations of the OH-stretching region in the FTIR spectrum of this sample, shown in Figure S4. SEM-EDS was performed with a JEOL 7001F FESEM using an accelerating voltage of 15 kV and a probe current of 13 nA. The samples were coated with 2 mm Ir and polished using mineral oil at 240, 30, 400, 600, 800, and 12000 grit SiC paper then using a 1 micrometer diamond/glycerol solution.

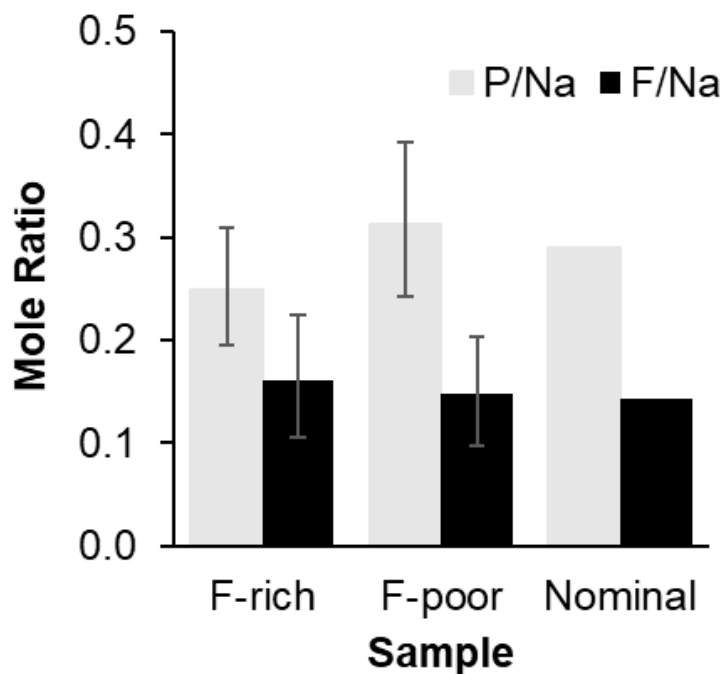


**Figure S2.** Summary of the mole ratios of P/Na and F/Na from the region selected for quantification of composition in the F-rich and F-poor sample with SEM EDS. The nominal mole ratios assuming the natrophosphate composition is  $\text{Na}_7(\text{PO}_4)_2\text{F}\cdot 19\text{H}_2\text{O}$  are also shown. The error bars are drawn at 2 standard deviations (95% confidence interval). The lack of dependence of the composition of natrophosphate to the synthesis of this compound in either F-rich or F-poor solutions is consistent with prior research using ion chromatography.<sup>1</sup>

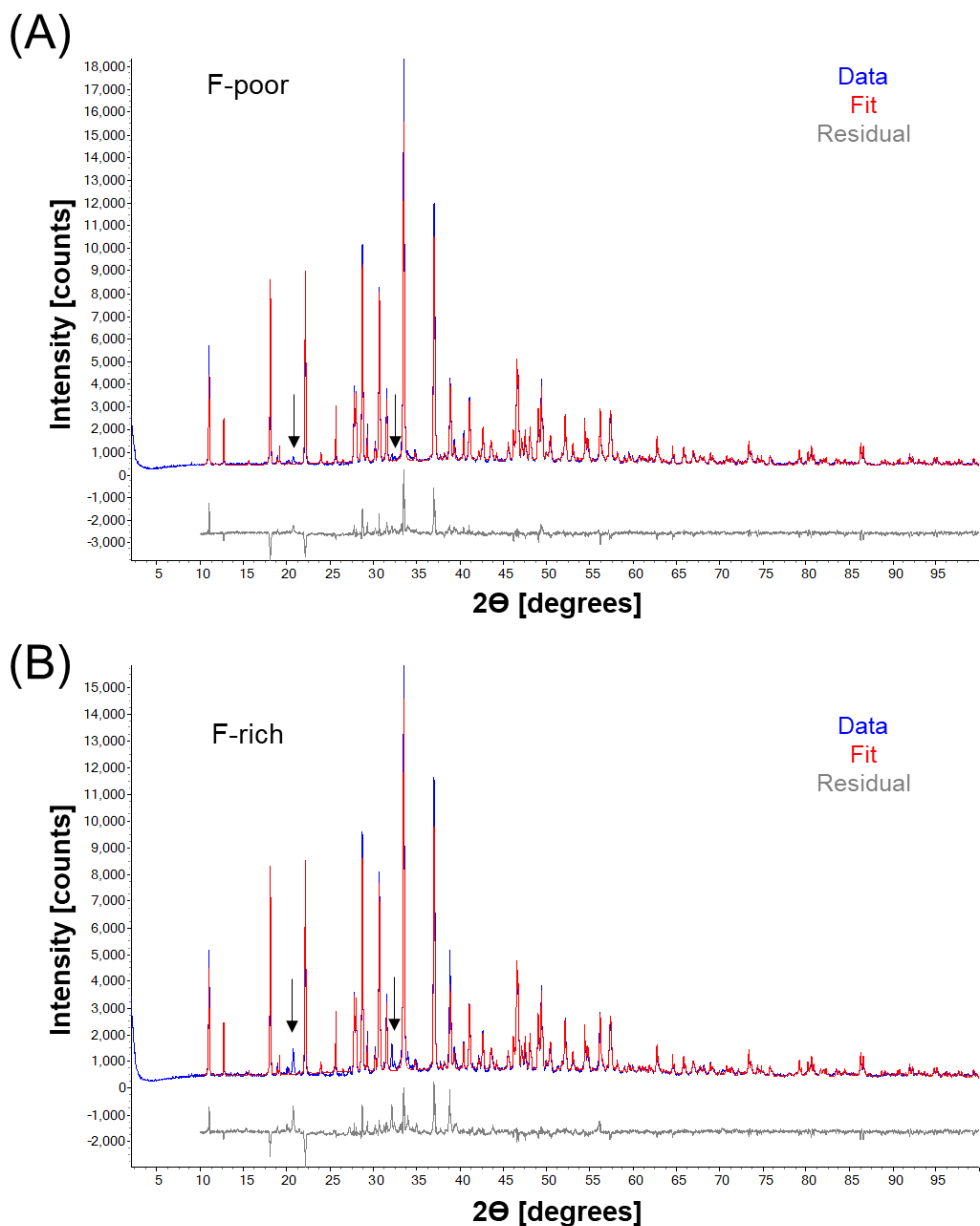


**Figure S3.** Subsequent X-ray diffraction characterizing the same two batches of natrophosphate synthesized under F-poor and F-rich conditions after 2 years of storage at 20°C in a sealed cryogenic vial (2 mL, Corning, internal thread/washer/self-stand) under N<sub>2</sub> in an N<sub>2</sub>-filled glovebox. (A) The diffractogram of the F-poor sample and (B) the diffractogram of the F-rich sample. Analysis of the results indicates that (1) finer homogenization of the sample can improve the quality of fit of the Rietveld refinement and (2) slight sample decomposition occurs after 2 years of storage based on the presence of new XRD reflections. Two resolved, XRD reflections are annotated with an arrow. Note that while the decomposition of natrophosphate is outside the scope of this manuscript, the residual could not be solely fit through the addition of a single phase (e.g. sodium orthophosphate, protonated sodium phosphate, sodium carbonate, nor sodium fluoride, nor hydrates of these phases) to natrophosphate. Quantities enumerating the quality of the fit are shown in Table S1. The fit using only natrophosphate is shown.

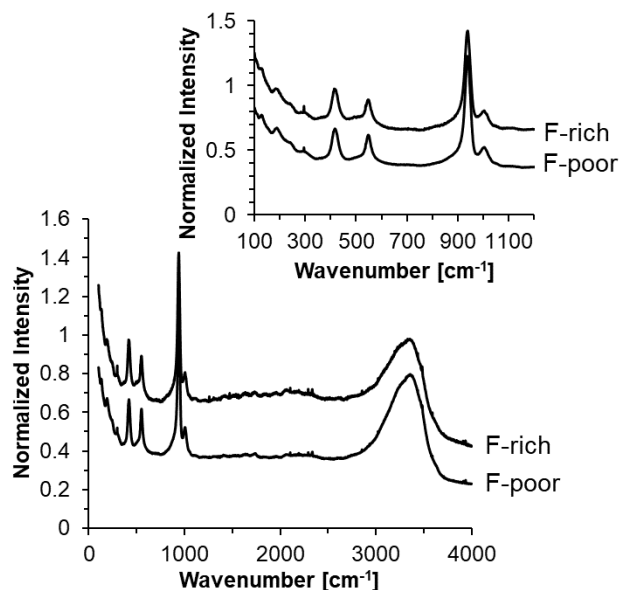


**Figure S4.** Raman spectra of natrophosphate synthesized in an F-rich and F-poor solution condition between wavenumbers of 100 and 4000 cm<sup>-1</sup>. The inset shows the low wavenumber region where bands attributed to the PO<sub>4</sub><sup>3-</sup> ion occur.

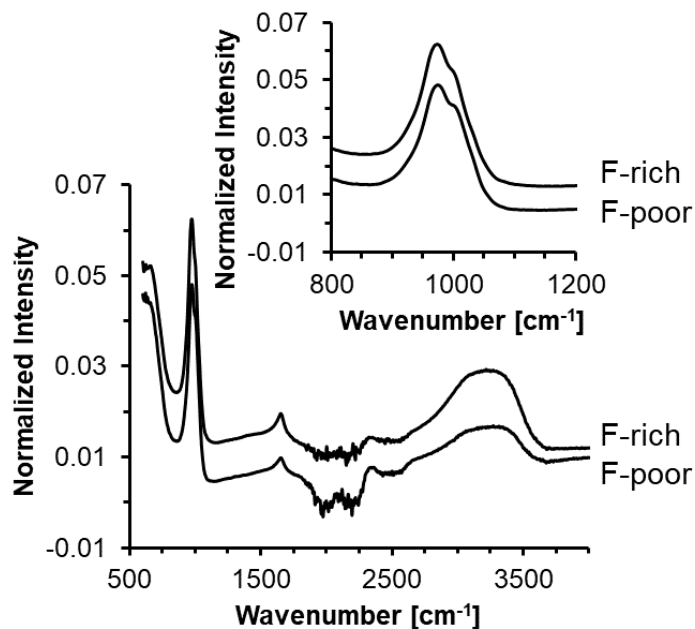


**Figure S5.** FTIR spectra of natrophosphate synthesized in an F-rich and F-poor solution condition between wavenumbers of 100 and 4000 cm<sup>-1</sup>. Note that the increase in the intensity of the water bending mode at 1600 cm<sup>-1</sup> and the OH stretching mode at 3200 cm<sup>-1</sup> in NaF1 is attributed to residual mother liquor. The inset shows the prominent bands near 1000 cm<sup>-1</sup> that are attributed to the PO<sub>4</sub><sup>3-</sup> ion.

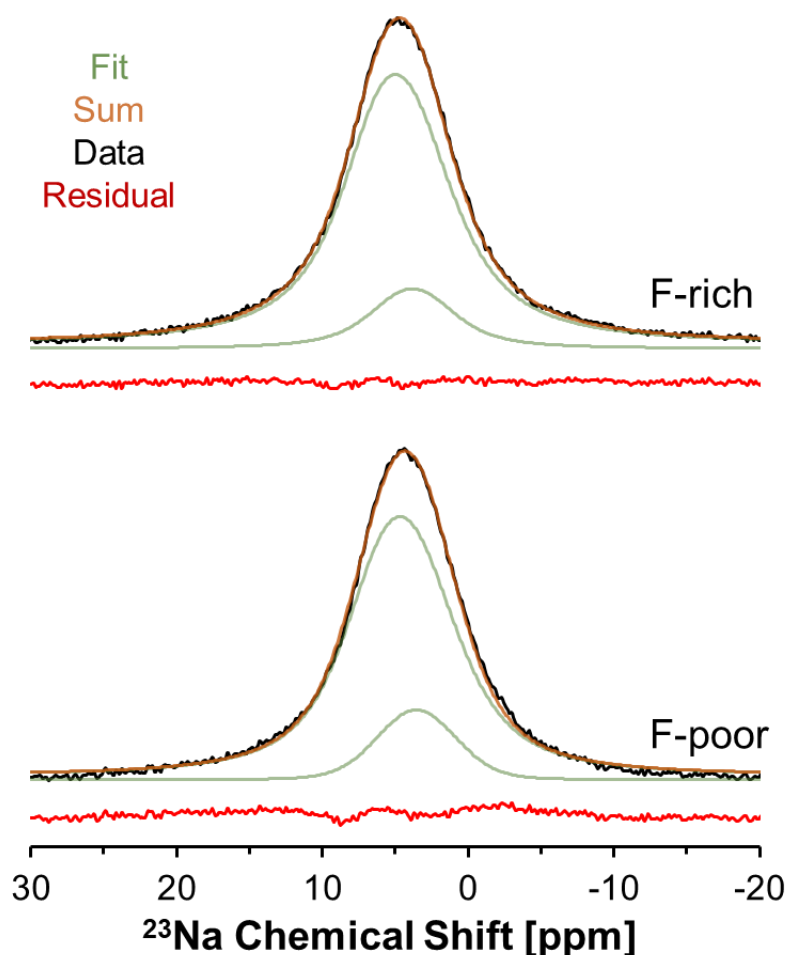


**Figure S6.**  $^{23}\text{Na}$  MAS NMR spectra of natrophosphate synthesized within an F-rich or F-poor solution. The  $^{23}\text{Na}$  MAS NMR spectra were acquired at a field strength of 7.05 T, with a 4 mm HXY probe operating in double resonance mode, and a spinning rate of 8 kHz. A  $0.5\ \mu\text{s}$  excitation pulse (50 kHz) equivalent to a  $\pi/20$  pulse calibrated on a 1 M NaCl sample was used to acquire the spectra. The chemical shifts were referenced to the resonance of the 1 M NaCl sample ( $\delta = 0$  ppm). The number of transients was 128, the acquisition time was 37.6 ms, the sweep width was 227273 Hz, and 8544 complex points were collected. The recycle delay was 1 s, which was sufficiently long to avoid saturation effects based on analysis of an array of spectra in which the recycle delay was varied and the peak intensity was monitored. The data were processed in Mestrenova, where 2 Hz of exponential line broadening were used and the free induction decays were zero-filled to 32658 complex points. The data was then fit using quadrupolar line shapes in ssNAKE. The values for the isotropic chemical shift, quadrupolar coupling coefficient, asymmetry parameter, and relative site abundances from the data acquired at 14.1 T were used and the Gaussian and Lorentzian broadening was varied because the two  $^{23}\text{Na}$  sites of natrophosphate were not resolved at 7.05 T. The quadrupolar line shape parameters are reported in Table S7. The lack of quadrupolar structures in the resonances at 7.05 T are consistent with the low quadrupolar coupling coefficient (under 1 MHz) found in the fitting of the  $^{23}\text{Na}$  MAS NMR spectra acquired at 14.1 T.

## 2.0 TABLES

**Table S1.** X-ray diffraction fitting data corresponding to Figure S3.

Sample	a [angstroms]	size [nm]	GOF	Bragg-R [%]	Rp [%]	Rwp [%]
F-poor	27.764	195(4)	3	7	7	9
F-rich	27.764	199(6)	3	7	8	11

**Table S2.**  $^1\text{H}$  MAS NMR Lorentzian Line Shape Parameters

Sample	Chemical Shift [ppm]	Full Width at Half Maxima [Hz]	Relative Integral [%]
F-rich	5.86	4270	100
F-poor	5.89	4331	100

**Table S3.**  $^{19}\text{F}$  MAS NMR Lorentzian Line Shape Parameters

Sample	Chemical Shift [ppm]	Full Width at Half Maxima [Hz]	Relative Integral [%]
F-rich	-222.77	273	100
F-poor	-222.73	270	100

**Table S4.**  $^{31}\text{P}$  MAS NMR Lorentzian Line Shape Parameters

Sample	Chemical Shift [ppm]	Full Width at Half Maxima [Hz]	Relative Integral [%]
F-rich	7.64	272	25.0
F-rich	8.34	136	75.0
F-poor	7.72	277	25.0
F-poor	8.31	137	75.0

**Table S5.**  $^{23}\text{Na}$  MAS NMR Quadrupolar Line Shape Parameters at 14.1 T

Sample	Isotropic Chemical Shift [ppm]	Quadrupolar Coupling Coefficient [MHz]	Asymmetry Parameter	Gaussian [Hz]	Lorentzian [Hz]	Relative Integral [%]
F-rich	7.94	0.88	0*	172.6	61.17	85.7
F-rich	4.44	0.40	0*	177.9	130.4	14.3
F-poor	7.98	0.89	0*	174.6	65.59	85.7
F-poor	4.40	0.38	0*	177.1	122.9	14.3

(\*) Due to the lack of fine quadrupolar line shape features on the  $^{23}\text{Na}$  MAS NMR spectra, the asymmetry parameter was fixed at a value of 0.

**Table S6.**  $^{23}\text{Na}$  MAS NMR Quadrupolar Line Shape Parameters at 7.05 T

Sample	Isotropic Chemical Shift [ppm]	Quadrupolar Coupling Coefficient [MHz]	Asymmetry Parameter	Gaussian [Hz]	Lorentzian [Hz]	Relative Integral [%]
F-rich	7.94*	0.88*	0*	128.4	512.5	85.7*
F-rich	4.44*	0.40*	0*	321.2	331.7	14.3*
F-poor	7.69*,#	0.89*	0*	260.7	425.5	85.7*
F-poor	4.11*,#	0.38*	0*	462.9	76.16	14.3*

(\*) The isotropic chemical shift, quadrupolar coupling coefficient, asymmetry parameter, and relative integral were fixed to values acquired at 14.1T, and the Gaussian and Lorentzian broadening was varied to fit the data acquired at 7.0T.

(#) The isotropic chemical shift of the two  $^{23}\text{Na}$  sites in the F-poor natrophosphate sample were both shifted by 0.29 ppm from the values acquired at 14.1 T. The shift in the isotropic chemical shift of these two sites at 7.0 T is likely due to a magnetic field drift, since the difference in the isotropic chemical shift between the two sites is conserved.



### 3.0 REFERENCES

- 1 D. L. Herting and J. G. Reynolds, The composition of natrophosphate (sodium fluoride phosphate hydrate), *Environ. Chem. Lett.*, 2016, **14**, 401–405, DOI: 10.1007/s10311-016-0574-2.